

Endocytic adaptors Arh and Dab2 control homeostasis of circulatory cholesterol

Wensi Tao,¹ Robert Moore, Yue Meng, Elizabeth R. Smith, and Xiang-Xi Xu²

Department of Cell Biology, Molecular Cell and Developmental Biology Graduate Program, Sylvester Comprehensive Cancer Center, University of Miami Miller School of Medicine, Miami, FL 33136

Abstract High serum cholesterol (hypercholesterolemia) strongly associates with cardiovascular diseases as the atherogenic LDLs promote atheroma development in arteries (atherosclerosis). LDL clearance from the circulation by LDL receptor (LDLR)-mediated endocytosis by hepatic and peripheral tissues and subsequent feedback regulation of endogenous synthesis of cholesterol is a key determinant of serum LDL level. Human mutation analysis revealed that autosomal recessive hypercholesterolemia (ARH), an LDLR endocytic adaptor, perturbs LDLR function and thus impacts serum cholesterol levels. In our genetic analysis of mutant mice, we found that deletion of another LDLR endocytic adaptor, Disabled-2 (Dab2), only slightly affected serum cholesterol levels. However, elimination of both *arh* and *dab2* genes in mice resulted in profound hypercholesterolemia similar to that resulting from *ldlr* homozygous deletion. In the liver, Dab2 is expressed in sinusoid endothelial cells but not in hepatocytes. When deleting both Dab2 and Arh, HMG-CoA reductase level increased to the level similar to that of *ldlr* knockout. Thus, in the absence of Arh, Dab2 in liver endothelial cells regulates cholesterol synthesis in hepatocytes. We conclude that the combination of Arh and Dab2 is responsible for the majority of adaptor function in LDLR endocytosis and LDLR-mediated cholesterol homeostasis.—Wensi, T., R. Moore, Y. Meng, E. R. Smith, and X-X. Xu. Endocytic adaptors Arh and Dab2 control homeostasis of circulatory cholesterol. *J. Lipid Res.* 2016. 57: 809–817.

Supplementary key words autosomal recessive hypercholesterolemia • Disabled-2 • low density lipoprotein • low density lipoprotein receptor • endocytic trafficking • serum cholesterol

Cholesterol is a major component of animal cell membranes as well as the starting substrate of steroid hormones. The homeostasis of this important and essential lipid is maintained by feedback regulation and transportation between tissues through the circulation (1). Serum cholesterol level is

a validated predictor of cardiovascular diseases (2, 3), and reduction of errant circulatory cholesterol level by inhibition of its synthesis using statins has been established as a highly successful intervention to reduce mortality from coronary artery diseases (4, 5). The balance of serum cholesterol level is determined by dietary intake, synthesis, and catabolism (6–8). The main carriers of atherogenic circulating cholesterol in humans are the LDL particles, which are produced mainly by the liver to deliver cholesterol to peripheral tissues; hepatic cells also play major roles in removing LDL from the circulation (6–8). Excessive cholesterol in the circulation, upon uptake by the liver via LDL receptor (LDLR)-mediated endocytosis, suppresses endogenous synthesis of cholesterol in the liver (6–8).

The studies of human mutations causing hypercholesterolemia and its associated pathologies have led to the understanding of cholesterol and LDL metabolism (9). The LDLR is a key determinant of serum cholesterol homeostasis, because individuals with extremely high serum cholesterol were found to have defective LDLR function (10, 11). Identification of mutations in LDLR that eliminate the production of the protein or render the receptor unable to undergo endocytosis attests that the LDLR is pivotal in the uptake and removal of LDL from the circulation by both hepatic and peripheral tissues (10, 11). Additional genetic analysis of kindreds afflicted with autosomal recessive hypercholesterolemia (ARH) led to the identification of the LDLR endocytic adaptor protein LDLRAP1/ARH (11). Another group of human mutations for autosomal dominant hypercholesterolemia was identified in the gene *PCSK9* (12), which encodes a proprotein convertase that binds LDLR and alters its endocytic trafficking and stability (13, 14). *PCSK9* mutations causing high serum LDL are gain of function, and loss-of-function

The work was supported by Office of Extramural Research, National Institutes of Health Grants R01 CA095071, R01 CA79716, and R01 CA75389, and by a pilot fund award from the Scientific Award Committee of the University of Miami Miller School of Medicine. The content is solely the responsibility of the authors and does not necessarily represent the official views of the National Institutes of Health.

Manuscript received 25 August 2015 and in revised form 15 March 2016.

Published, JLR Papers in Press, March 22, 2016
DOI 10.1194/jlr.M063065

Copyright © 2016 by the American Society for Biochemistry and Molecular Biology, Inc.

This article is available online at <http://www.jlr.org>

Abbreviations: ARH, autosomal recessive hypercholesterolemia; Dab2, Disabled-2; DAPI, 4',6-diamidino-2-phenylindole; HMGCR, HMG-CoA reductase; LDLR, LDL receptor; MEF, mouse primary embryonic fibroblast; PCSK9, proprotein convertase subtilisin/kexin type 9; PECAM, platelet endothelial cell adhesion molecule; VLDLR, VLDL receptor.

¹Present address of W. Tao: Bascom Palmer Eye Institute, Department of Ophthalmology, University of Miami Miller School of Medicine, Miami, FL 33136.

²To whom correspondence should be addressed.
e-mail: xxu2@med.miami.edu

mutations were also identified in individuals with peculiarly low serum cholesterol (15). Small-molecule and antibody blockage of PCSK9 have now been developed and tested, showing promise as effective LDL cholesterol-lowering drugs (16, 17).

The role of ARH in recruiting LDLR into clathrin-coated vesicles in endocytosis has been studied in cultured cells (18), and the impact on circulating cholesterol has been investigated in mutant mice (19–21). Another endocytic clathrin adaptor, Disabled-2 (Dab2), is potentially an LDLR-selective adaptor (22). The activity and ability of Dab2 to mediate LDLR endocytosis have been demonstrated in cultured cells (23). However, Dab2-deficient mice have only minor changes in serum cholesterol level (24), and the involvement of Dab2 in cholesterol metabolism in intact animals is uncertain.

The autosomal dominant familiar hypercholesterolemia caused by inactivating mutations in the *LDLR* gene exhibits a greater serum LDL level and higher degree of severity of the symptoms than found with mutations in *ARH* gene (11). Analysis of mutant mice also showed that serum cholesterol is much higher in LDLR-null than in *arh*-deleted mice (19–21, 25). Presumably, additional endocytic adaptors other than Arh may support LDLR endocytosis. Conventional *dab2* gene deletion in mice results in early embryonic death (26–28). We generated a conditional knockout line and were able to produce Dab2-null mice to study their postnatal phenotypes (24). Here, we investigated the relative importance of Dab2, another endocytic adaptor capable of binding to LDLR (22), in LDLR-mediated clearance of circulating LDL and the regulation of cholesterol synthesis.

MATERIALS AND METHODS

Sources and maintenance of mutant mice

A line of *dab2* floxed mice previously constructed by the lab was used throughout this study (24). Female *dab2* (fl/fl) and male *dab2* (+/df):Sox2-Cre mice were used as breeding pairs. Among the progenitors, *dab2* (fl/df):Sox2-Cre were conditional knockouts shown to be essentially Dab2 null after birth, while *dab2* heterozygous [*dab2* (+/df):Sox2-Cre] and floxed [*dab2* (+/fl)] mice were designated as controls.

The *arh* knockout mice (B6;129S-Ldlrap1tm1Her/J) (19) and *ldlr* knockout mice (B6.129S7-Ldlrtm1Her/J) (25) were purchased from Jackson Lab. Dab2 conditional knockout mice (24) were bred into the *arh* knockout background as described in the strategy.

Mice were routinely maintained on a regular enriched diet, 5K20 chow (10% fat; LabDiets Inc.). A high-sucrose diet (no. 960237; MP Biomedicals) containing 60.2% sucrose and 20% casein, 15% cellulose, 0.3% DL-methionine, 3.5% minerals and vitamins, and <0.2% fat was used as a high-caloric-diet regimen for 3 months to induce hypercholesterolemia. Animals were housed on a 12:12 h light-dark cycle with ad libitum access to food and water. The Institutional Animal Care and Use Committee reviewed and approved all the experimental procedures using laboratory mice described in this study.

Genotyping of mutant mice

The PCR genotyping of *ldlr* knockout (25) and *dab2* conditional knockout (24) mice was performed following the previously published protocols.

Since the original *arh* mutant allele contains a neomycin-resistant cassette flanked by two LoxP sites (19), the genotyping procedure was modified to distinguish the original *arh*^{RO} as well as *arh*^{deltaflox}, in which two LoxP sites were removed by Cre recombinase. Genotyping PCRs were performed with all primers at 1 μ M concentration using the master mix from Denville Scientific. Four primers were used in the PCR reactions: mArhF3 (5' GTG TTC AGA GGA GAG GAA CT 3'); mArhR3 (5' CTG GTG TGC AGT TAG GTT CA 3'); XU2010-01 (5' CTG CAG ACA AGA TGC ACG AC 3'); and Neo-36 (5' CAG GAC AGC AAG GGG GAG GAT TGG G 3'). The parameters for the genotyping PCR program were as follows: 5 min at 94°C; 30 cycles (30 s at 94°C, 30 s at 57°C, 3 min at 72°C); 10 min at 72°C; and 4°C overnight. The predicted sizes of the amplicons are the following: wild-type, 650 bp; *arh*^{KO}, 380 bp; and *arh*^{deltaflox}, 300 bp. In this report, the genotypes of the mutant mice and derived cells are designated as *arh* (+/–) or *arh* (–/–).

For the nomenclature of *dab2* mutant mice, “fl” and “df” were used to indicate conditional and deleted alleles, respectively. Mutant mice and tissues derived from Sox2-Cre-mediated deletion are denoted as “HET” and “CKO.” Mouse primary embryonic fibroblast (MEF) cells were genotyped directly following expansion in cultures and are noted as *dab2* (+/+), (+/–), or (–/–).

Profiling of serum lipids

Mice were fasted for 4–6 h and then anesthetized prior to tissue collection. Blood was collected by cardiac puncture, and the tissues and fats to be examined were dissected and collected. To obtain serum, blood samples were allowed to clot at room temperature for 15 min, and the serum was collected following centrifugation for 10 min at maximum speed in a bench-top clinical centrifuge and stored at –80°C until use. Lipid chemistry analysis was performed using an automated Vitros 250 chemistry analyzer (Johnson and Johnson) by the University of Miami Comparative Pathology Laboratory Core. The levels of serum cholesterol, triglyceride, and HDL were determined colorimetrically. LDL and VLDL levels were estimated with the following formulae: VLDL = 1/5 of triglycerides; LDL = total cholesterol – (HDL + VLDL).

Extraction and measurement of cholesterol in tissues

Cholesterol was extracted from liver samples according to the Folch method (29). Briefly, liver tissue was lysed in RIPA buffer and homogenized with glass beads. A total of 10 mg protein was added to 10 vol of an extract solvent containing chloroform-methanol (2:1, v/v). Monoacylglycerols (100 pmol) and acylethanolamides (100 pmol) were added to each sample as internal standards. Following vortexing to extract the lipids, the mixtures were centrifuged at 5,000 *g* for 10 min. The lipid extracts in the chloroform (lower phase) were collected, and chloroform was vaporized under vacuum with a gentle flow of nitrogen gas. The samples were analyzed by LC/MS in the Lipidomics Core of Rutgers University (http://dixonlab.rutgers.edu/pages/lc_ms_facility).

Preparation of primary cells

MEFs were isolated from E12.5 embryos generated from designated genotypes (24). Briefly, the head of dissected embryos was first removed and used for PCR genotyping, and the remainder was minced using a scalpel. After incubation for 10 min in 0.25% trypsin at 37°C, the cells were pelleted by a brief centrifugation and plated in a T75 flask in DMEM media supplemented with 10% FBS. The cells from the embryonic outgrowths were harvested and expanded. Western blot analysis of the cells was used to confirm the genotype obtained from PCR of the head tissues.

Western blots and immunofluorescence microscopy

For Western blot analysis, cells were washed twice with cold PBS and collected in RIPA buffer (20 mM Tris pH 7.5, 50 mM NaCl,

0.1% SDS, 0.5% sodium deoxycholate). The samples were then lysed in SDS gel loading buffer and boiled for 10 min. The proteins were separated on 8% SDS-polyacrylamide gels and transferred from the gels to the nitrocellulose membranes. The membranes with proteins samples were used for Western blot analysis.

For immunofluorescence microscopy, tissue were fixed in 4% paraformaldehyde in PBS, cryopreserved in 30% sucrose, and embedded in OCT. Cryosections of 10 μ m thickness were subjected to antigen retrieval with 1% SDS and then incubated with specific primary antibodies. Fluorescently conjugated antibodies directed against the appropriate species of primary antibodies were used as secondary antibodies (24, 30).

Primary antibodies used include the following: anti-Dab2 (1/5,000) (BD Transduction Laboratories; 610465), anti-Dab2 rabbit polyclonal (TMD) antibody (24, 28, 30) (1 in 1,000), anti-Beta-actin (1/5,000) (BD Transduction Laboratories; 612657), anti-ARH (1/2,000) (Santa Cruz; sc-100653), anti-LDLR (1/1,000) (Novus Biologicals; EPI1553Y), and anti-adaptin α (BD-Bioscience; 610502), rabbit anti-HMG-CoA reductase (HMGCR) antibody (AbCam; ab174830), rat anti-F4/80 (mouse) antibody (AbCam; ab6640), and rat anti-mouse CD31 [platelet endothelial cell adhesion molecule (PECAM)-1] (BD Biosciences; 550274).

The secondary antibodies for Western blotting were conjugated with HRP and were used (1/5,000 dilution) following the instructions from the manufacturer (rabbit and mouse secondary antibodies were from BioRad; goat secondary antibodies were from Jackson ImmunoResearch). SuperSignal West Extended

Duration Substrate (Pierce Biotech) was used for chemoluminescence detection of specific proteins.

Assay for LDL uptake by cells in cultures

MEFs were prepared from control and mutant mice with various genotypes as described previously (24). Cells were maintained in DMEM media supplemented with 10% FBS. The cells were switched to the DMEM media containing 5% lipoprotein-deficient serum for 12 h prior to assay. A total of 25 μ g/ml human LDL particles labeled with BODIPY dye (Sigma Inc.) were added to the cells. After 5 h incubation, cells were washed twice with PBS and fixed in 4% paraformaldehyde. DAPI (4',6-diamidino-2-phenylindole) was used as a nuclear counterstain. Images were acquired using a Zeiss Z1 inverted microscope operated by AxioVision software.

Quantitative RT-PCR for the analysis of gene expression

Total RNA was harvested from MEF cells using the Qiagen RNAeasy kit. cDNAs were prepared from the extracted RNA by reverse transcription with iScriptTM cDNA Synthesis Kit according to the manufacturer's instructions (BioRad). Quantitative RT-PCR was performed using CFX ConnectTM Real-Time PCR Detection System with 2 \times SYBR[®] Green Supermix and specific primers. Target gene quantification is reported with normalization to the signals obtained from reference gene GAPDH. The primers used were as follows: LDLR forward sequence, 5' CTG GAC CGG AGC GAG TAC AC 3'; LDLR reverse sequence, 5' GAC GCC GTG GGC

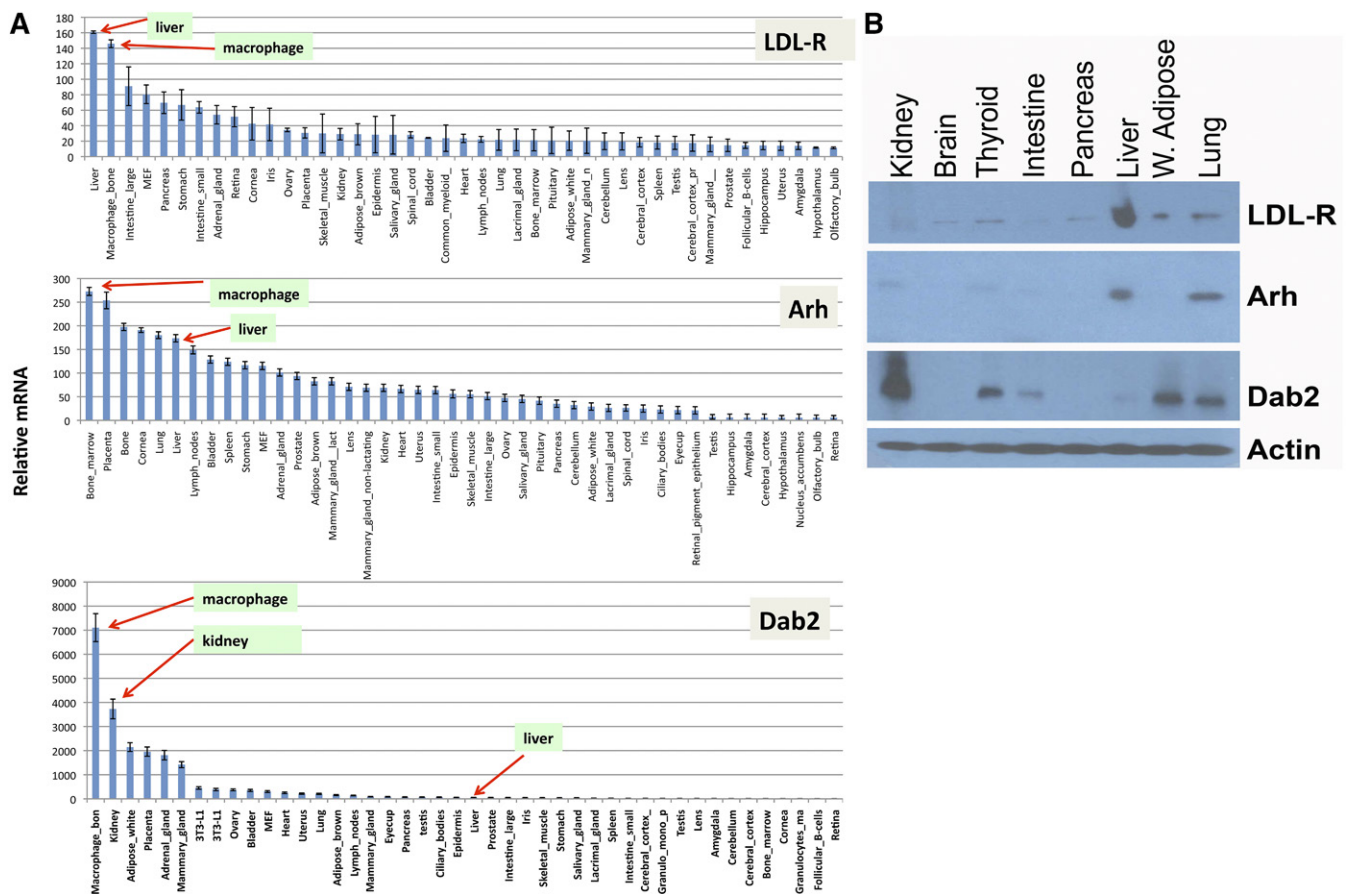


Fig. 1. Expression spectrum of Dab2, Arh, and LDLR mRNA in murine tissues. A: Microarray data sets were acquired from an online public data set GeneAtlas MOE430, gcrma (<http://biogps.org/#goto=genereport&id=13132>). The high-throughput gene expression profiling for Dab2, Arh, and LDLR was generated from a diverse array of normal tissues, organs, and cell lines from mice. The final readouts were averages of four different probe sets with SEM shown as error bars, normalized to housekeeping genes, and ranked according to the abundance of mRNA expression. B: Selective tissues were harvested from 3-month-old mice, and lysates were prepared for Western blot analysis.

TCT GT 3'; VLDL receptor (VLDLR) forward sequence, 5' AAC CAA GAG GAA GTT CCT GTT TAA CT 3'; VLDLR reverse sequence, 5' TGA CCA GTA AAC AAA GCC AGA CA 3'; GAPDH F49 sequence, 5' GGT GAA GGT CGG TGT GAA CG 3'; and GAPDH R281 sequence, 5' CTC GCT CCT GGA AGA TGG TG 3'.

RESULTS

We first surveyed the mRNA expression profile of LDLR, Arh, and Dab2 in mouse tissues and cell lines by analysis of GeneAtlas public data set. Liver is the top site among all tissues for which both LDLR and Arh are highly expressed, though both LDLR and Arh are widely expressed among other tissues albeit at lower levels (11) (Fig. 1). This is consistent with that liver is the main site for LDLR-mediated clearance of LDL particles, and Arh acts as the main endocytic adaptor. In comparison, Dab2 is expressed highly in several tissues and cell types including macrophages, kidney,

white adipose, adrenal, lactating mammary glands; however, the expression, although present widely, is much lower in magnitude in other tissues including the liver (Fig. 1A). The presence of proteins were validated by Western blot of tissues obtained from experimental mice, and the results indicate that LDLR and Arh proteins are indeed abundant in liver, whereas Dab2 is much lower in the liver compared with other tissues analyzed (Fig. 1B).

Although *arh* knockout mice have substantially increased circulatory cholesterol, the level is significantly lower (~30%) than that of the *ldlr* knockout (19, 20). Dab2-null mice generated using Sox2-Cre to delete the floxed *dab2* locus have a small increase in serum cholesterol (24). We designed a strategy to produce Dab2 and ARH double-knockout mice by crossing *dab2* (fl/fl), Sox2-Cre transgenic, and *arh* (-/-) mice (Fig. 2A). Sox2-Cre is highly efficient in deleting *dab2* gene in the embryo proper without eliminating *dab2* in extraembryonic tissues, and all *dab2* loci are depleted in

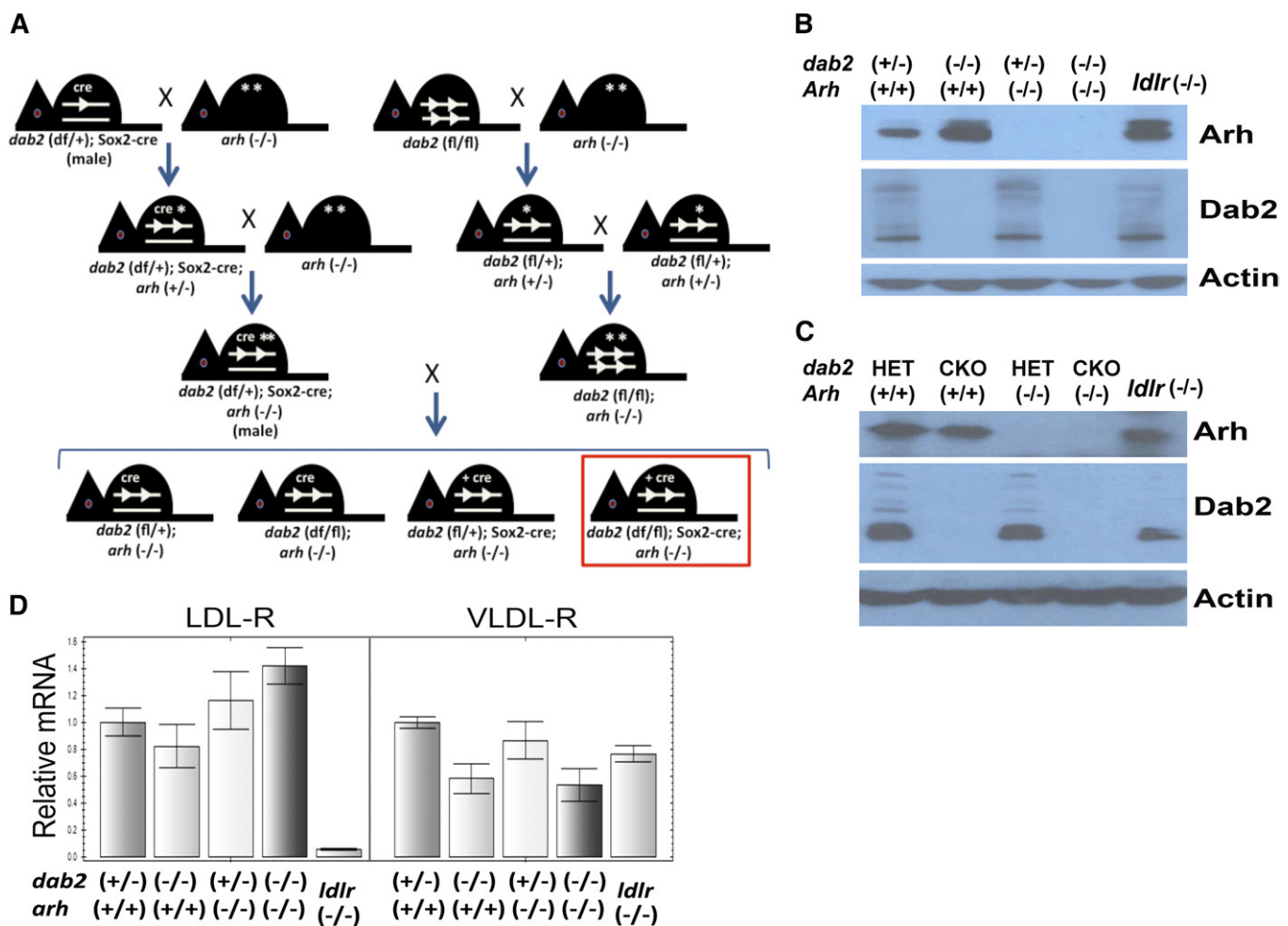


Fig. 2. Generation of Dab2 and Arh double-knockout mice. **A:** Mice from colonies of *dab2* flox, Sox2-Cre transgenic, and *arh* null were crossed to obtain compound Dab2- and *arh*-null mice. The *arh* mutant allele is noted as “*”. A three-step strategy was designed to produce the double-knockout mice: *dab2* (fl/df); Sox2-Cre; *arh* (-/-) (indicated with a red box). Only male mice carrying the Sox2-Cre transgene were used in the crosses to avoid transmission of the Cre protein through oocytes. **B:** MEFs were prepared from embryos with *dab2* (fl/df), *dab2* (df/df), *dab2* (fl/df); *arh* (-/-), *dab2* (df/df); *arh* (-/-), and *ldlr* (-/-) genotypes. The cells were expanded and genotyped to determine whether *dab2* statuses were (+/-) or (-/-). Cell lysates were prepared for Western blotting to assay for Dab2 and Arh proteins. **C:** Hepatic tissues were harvested from the mutant mice of 3 months of age. Total cell lysates were prepared and analyzed by Western blotting. The *dab2* genotypes from Sox2-Cre-mediated deletion were noted as HET or CKO. **D:** Expression of LDLR and VLDLR mRNA in *dab2*- and/or *arh*-deleted MEF cells. Quantitative real-time RT-PCT analysis of LDLR and VLDLR mRNA isolated from control and mutant MEFs was performed in triplicate and reported as means plus SEMs.

embryos by the E9.5 stage (24). Previously, we found that *dab2* wild-type and heterozygous mice are essentially indistinguishable in all physiological parameters tested (24); thus, *dab2* heterozygous siblings generated from the colonies were used as controls and substituted for true wild-type mice. Remarkably, *Dab2* and *Arh* double-knockout mice were produced in the expected Mendelian ratio and were grossly normal. Western blot analysis of MEFs and liver tissues derived from the control and mutant mice confirmed the complete absence of *Dab2* and *Arh* proteins in the compound mutant mice (Fig. 2B, C). Elimination of *Dab2* or *LDLR* elicited a compensatory increase in *Arh* protein in MEFs (Fig. 2B) but not in liver tissues (Fig. 2C). The increased *Arh* in MEFs also contains a modified form showing an increased apparent molecular mass (Fig. 2B). It was uncertain if these variants are related to the posttranslational modifications such as *S*-nitrosylation of *Arh* (31). In contrast, *arh* deletion did not cause a compensatory expression of *Dab2* or *LDLR* proteins in either MEFs or hepatic tissues (Fig. 2B, C). In MEFs, we also observed an increased *LDLR* mRNA in *Arh*-null cells and reduced *VLDLR* upon *dab2* deletion (Fig. 2D). Thus, a transcriptional regulatory network between the receptors and endocytic adaptors exists that warrants future investigation.

The matching control, *ldlr* ($-/-$), *dab2* (*df/df*) (or CKO), *arh* ($-/-$), and *Dab2*-*Arh* double-knockout mice were kept on a high-sucrose diet to compare the impact of

the genotypes on serum cholesterol level, following the experimental conditions used in the previous studies in *Arh* and *LDLR* knockout mice (19, 20). In such a situation, the source of circulatory cholesterol was solely from endogenous synthesis. On a normal chow diet, there were no noticeable differences between the body weights of wild-type, mutant, and double-knockout mice. However, on high-sucrose diet, mice with *dab2* deletion gained less body weight than *dab2* heterozygous (Fig. 3A). We found that the *dab2* and *arh* double-knockout mice had serum cholesterol elevated to a level similar to that of the *LDLR* knockout (Fig. 3B). The high serum cholesterol in the double-knockout mice appears to be a combination of increased cholesterol in LDL, HDL, and VLDL (Fig. 3B). Interestingly, the serum triglyceride level in the double-knockout mice increased, but not to the same level as in *LDLR* knockout mice (Fig. 3B). Increased accumulation of cholesterol in the livers of the double-knockout mice was also found quantitatively comparable to those of *LDLR* knockout (Fig. 3C).

The MEFs from control and knockout genotypes were assayed for their ability to uptake BODIPY-labeled LDL particles. Compared with *dab2* (+/-) cells, *Dab2*- or *Arh*-null cells had significant reduced ability to uptake LDL particles (Fig. 4A). Remarkably, the *Arh* and *Dab2* double-knockout cells had little ability to uptake LDL, of a level similar to that of *LDLR* null (Fig. 4). We quantified LDL

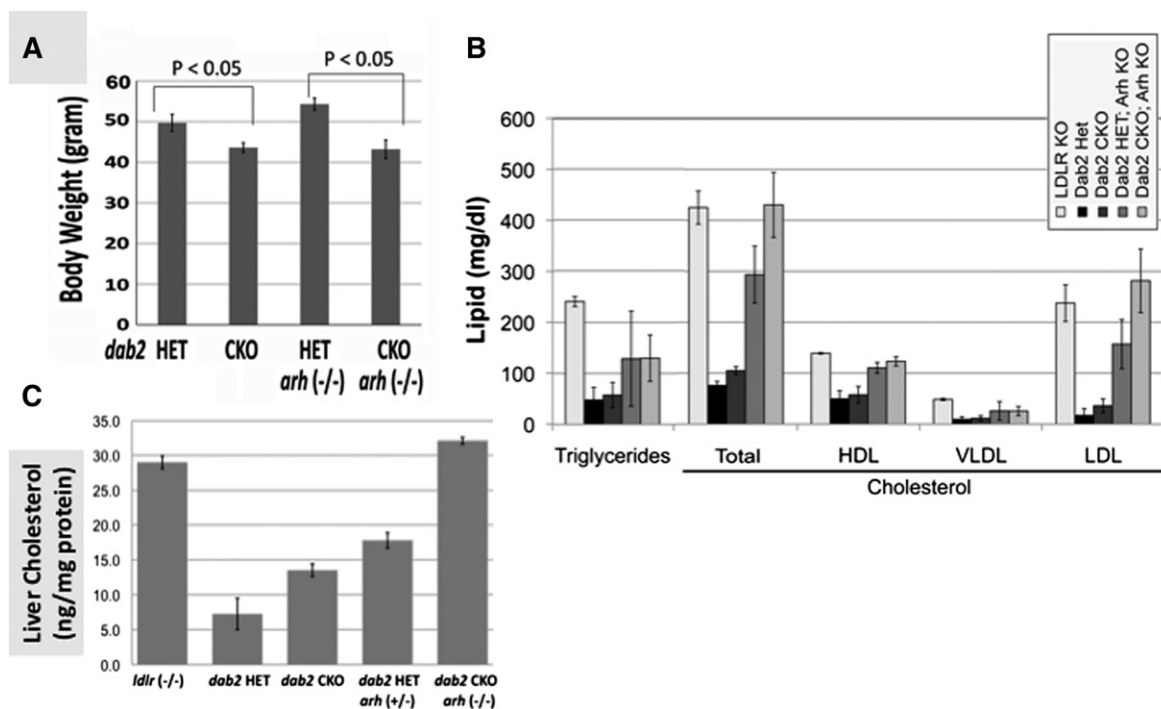


Fig. 3. Serum lipid profiles of control and mutant mice fed a high-sucrose diet. Control and mutant mice (12 mice in each category) were maintained according to identical procedures and conditions. For cholesterol measurement, the mice were provided with a cholesterol-free, high-sucrose diet (No. 960237; MP Biomedical: 60.2% sucrose, 20% casein, 15% cellulose, 0.3% DL-methionine, 3.5% mineral and vitamins, and 0.2% fat) at 3 weeks of age and continued to 3 months of age. A: Body weights were measured at the end of the experiments for each animal, the values from each cohort (6 mice each) of genotype were averaged, and SEMs were calculated. B: Serum from each mouse from a panel of 10 for each genotype was collected for quantification of lipid content, including total serum cholesterol, LDL cholesterol, triglycerides, HDL cholesterol, and VLDL. The average values with SEM are presented. The differences between values from *Dab2* or *Arh* individual knockout to those of double knockout were determined to be statistically significant by Student's *t*-test ($P < 0.005$). C: Liver tissues from individual mice from a panel of 10 for each genotype were collected for quantification of cholesterol content, and averages with SEM are shown. The differences between all the categories were determined to be statistically significant ($P < 0.005$).

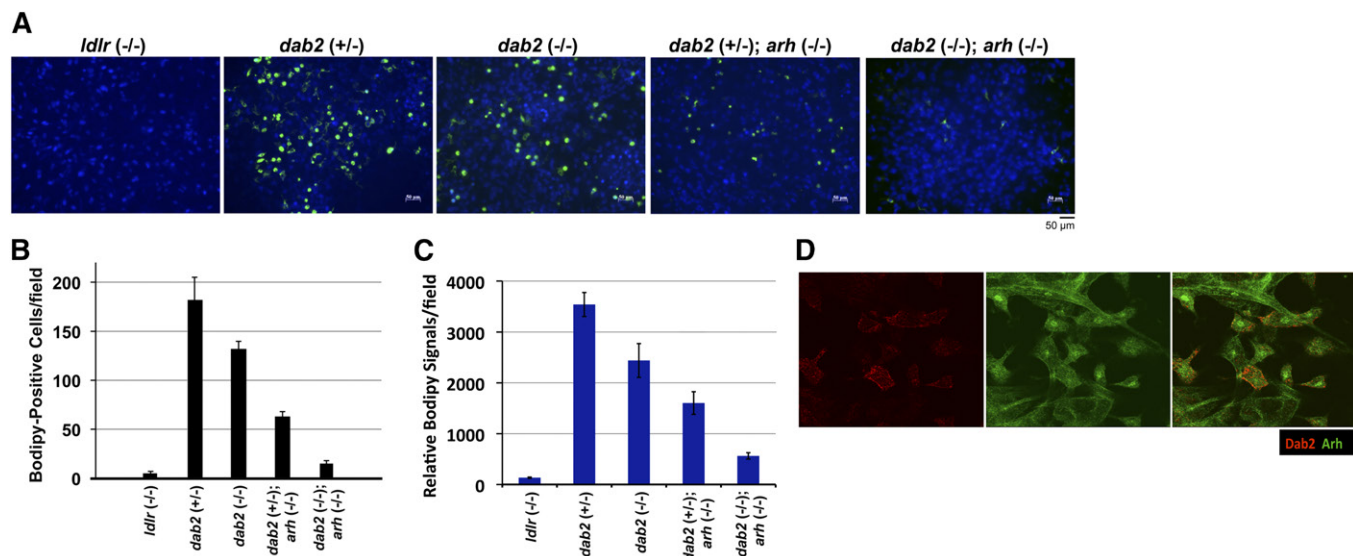


Fig. 4. LDL uptake by control and mutant MEFs. BODIPY-conjugated LDL particles at a concentration of 25 $\mu\text{g/ml}$ were incubated for 5 h with MEFs of control and mutant genotypes that were cultured in medium with 5% lipoprotein-depleted serum. The Dab2-deficient MEFs derived from Sox2-Cre-mediated deletion are denoted as *dab2* (-/-) or (+/-). A: BODIPY fluorescence images (green) of the cells were acquired using a Zeiss Z1 inverted microscope operated by AxioVision software. B: The fraction of BODIPY-positive cells of a defined area was quantified in triplicate, and the averages with SEM are shown. All categories had statistically significant differences ($P < 0.005$). C: The total BODIPY fluorescence signal in a defined field was quantified using Image J program in triplicate, and all categories had statistically significant differences. D: Wild-type MEFs were stained with antibodies to Dab2 (red) and Arh (green) for analysis using immunofluorescence microscopy.

uptake by either determining the number of BODIPY-positive cells (Fig. 4B) or by measuring the total BODIPY signal in a defined field (Fig. 4C). Interestingly, the values obtained from either measurement were similar. We further determined that Dab2 was heterogeneously expressed in the cell population, and only $\sim 30\%$ of the MEFs were Dab2 positive (Fig. 4D). Thus, cells positive for either Dab2 and/or Arh are sufficient to support LDLR-mediated uptake of BODIPY-labeled LDL and were fluorescently labeled to a similar extent; only the cells negative for both Dab2 and Arh remained unlabeled. The observation suggests that the dosage of LDLR adaptor protein is not a limiting factor for LDL uptake, and the presence of either Dab2 or Arh is sufficient, yet the presence of both adaptors is not additive in the same cell. Thus, the combination of Dab2 and Arh accounts for the majority of adaptor activity responsible for LDLR endocytosis and LDL uptake by MEFs, by presenting individual cells with either Arh and/or Dab2 as the endocytic adaptor for LDLR.

Cholesterol in these mice was exclusively endogenously produced because the high-sucrose diet lacked exogenous cholesterol. Thus, the increased serum cholesterol would be either because of a reduced uptake or an augmented synthesis/secretion. We measured HMGCR, the rate-limiting enzyme for cholesterol synthesis in liver tissues (Fig. 5). Arh and Dab2 double-knockout liver tissues had a greatly increased HMGCR level, comparable to that of LDLR knockouts (Fig. 5).

We also examined the cell type in which Dab2 is present in the liver. Surprisingly, Dab2 is not expressed in hepatocytes. The pattern of Dab2 staining by immunofluorescence microscopy resembles that of PECAM-1, also noted as CD31, a marker of liver sinusoidal endothelial cells

(Fig. 6A). Under higher magnification (Fig. 6A), the Dab2 signal appeared localized to most, but not all, endothelial cells in the liver. The liver tissue was LDLR positive throughout, with a slightly higher intensive along the sinusoidal endothelial edges (Fig. 6B). Additionally, we compared Dab2 with F4/80 staining, a marker of macrophages and Kupffer cells (Fig. 6C). The staining patterns were clearly dissimilar between Dab2 and F4/80 in the same section, and the two immunofluorescent signals were often seen adjacent but not colocalized (Fig. 6C), suggesting that Dab2 is not expressed in Kupffer cells. Thus, we conclude that Dab2 is expressed in the sinusoid endothelial cells but not in hepatocytes or Kupffer cells in the liver. This would suggest that Dab2 mediates a noncell autonomous activity to regulate hepatic HMGCR activity and cholesterol homeostasis.

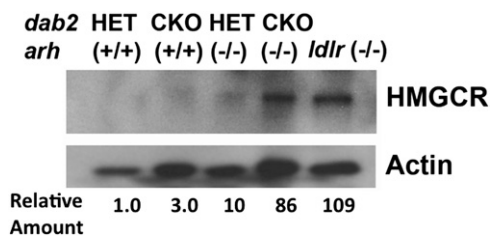


Fig. 5. Induction of liver HMGCR in Dab2 and Arh double-knockout mice. Hepatic tissues were harvested from the mutant mice of 3 months of age. Total cell lysates were prepared and analyzed by Western blotting for the expression of HMGCR. The signals from the blot were quantified using Image J program and a relative value for HMGCR was estimated with normalization using β -actin signal.

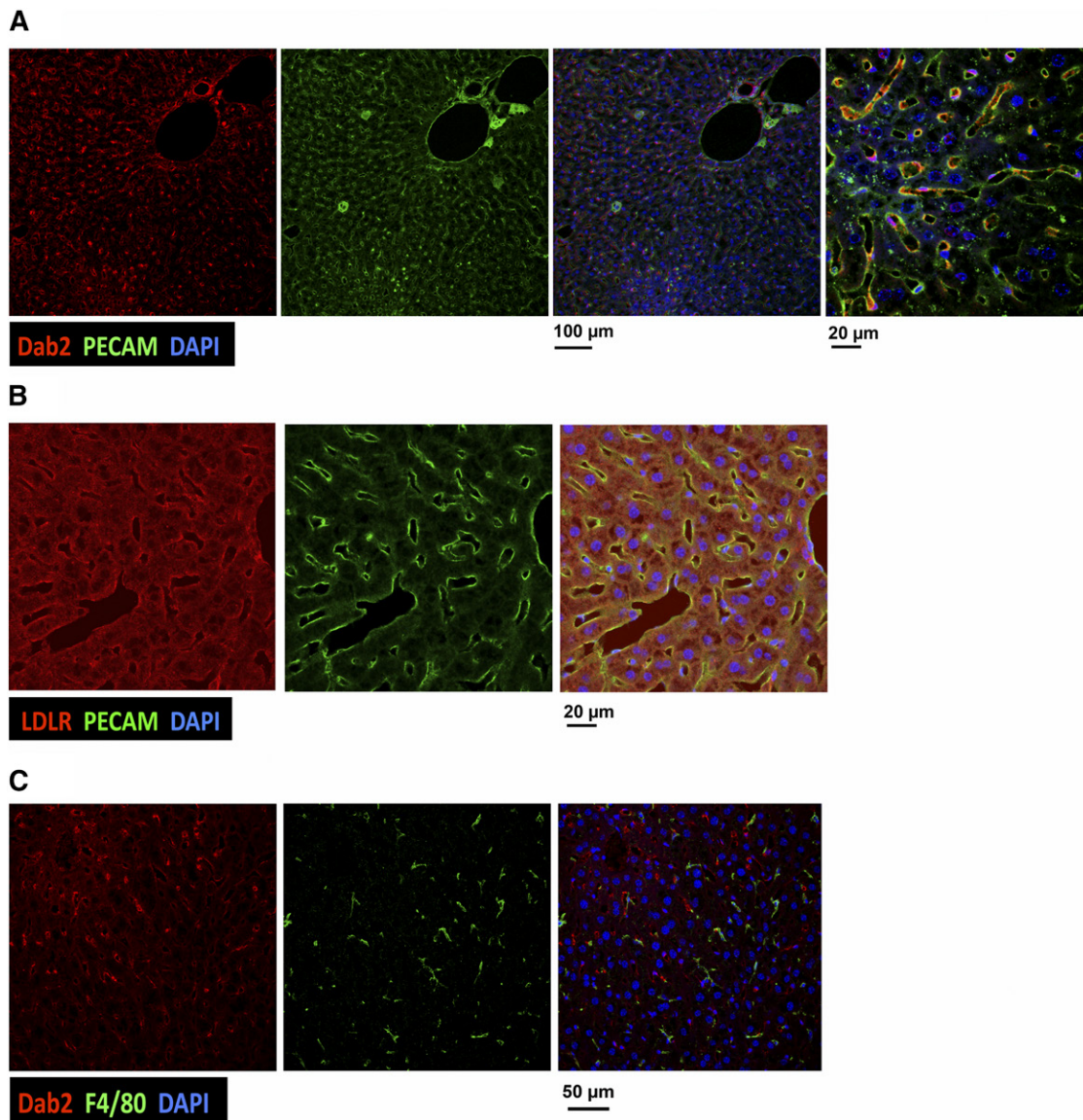


Fig. 6. Expression of Dab2 in the sinusoidal endothelial cells of the liver. Hepatic tissues were harvested from wild-type mice of about 3 months of age. The samples were prepared for cryosectioning, and the sections were placed on glass slides for immunofluorescence analysis using confocal microscopy. A: Liver sections were stained for Dab2 (red), PECAM (green), and DAPI (blue). An image at higher magnification is also shown (right panel). B: Liver sections were stained for LDLR (red), PECAM (green), and DAPI (blue). C: Liver sections were stained for Dab2 (red), F4/80 (green), and DAPI (blue).

At a greater magnification, the concentrated and punctate LDLR staining near the sinusoidal edge did not overlap with PECAM staining that marks the sinusoidal endothelial cells, as examples indicated by arrows (Fig. 7A). This is consistent with the notion that the majority of LDLR locates within hepatocytes rather than the endothelial cells. Similarly, Dab2 staining is distinct from the intense LDLR signals near the sinusoidal edge (Fig. 7B). However, partial overlapping of Dab2 and LDLR signals was observable (Fig. 7B, arrows). Thus, the majority of liver LDLR located within the hepatocytes is inaccessible to Dab2, which associates only with LDLR of the sinusoidal endothelial cells. Therefore, we conclude that Dab2-mediated LDLR endocytosis in the liver sinusoidal endothelial cells, which contain only a much lower level of LDLR, is able to regulate hepatic HMGCR expression and cholesterol synthesis.

DISCUSSION

The experiments described in this study show that double knockout of the endocytic adaptors Arh and Dab2 mirrored the phenotypes of the LDLR knockout, in the similar elevated level of circulating and liver cholesterol and increased hepatic HMGCR. Thus, we conclude that LDLR endocytic adaptors Arh and Dab2 control the LDLR-dependent regulation of the homeostasis of circulatory cholesterol, including both synthesis and removal (1). A model is proposed that the combined roles of Arh and Dab2 account for the adaptor function in LDLR endocytosis and cholesterol homeostasis in intact animals. We suggest that Arh is the main LDLR endocytic adaptor for clearance of circulating LDL in both liver and extrahepatic tissues. In the liver, Dab2 participates in LDLR-mediated

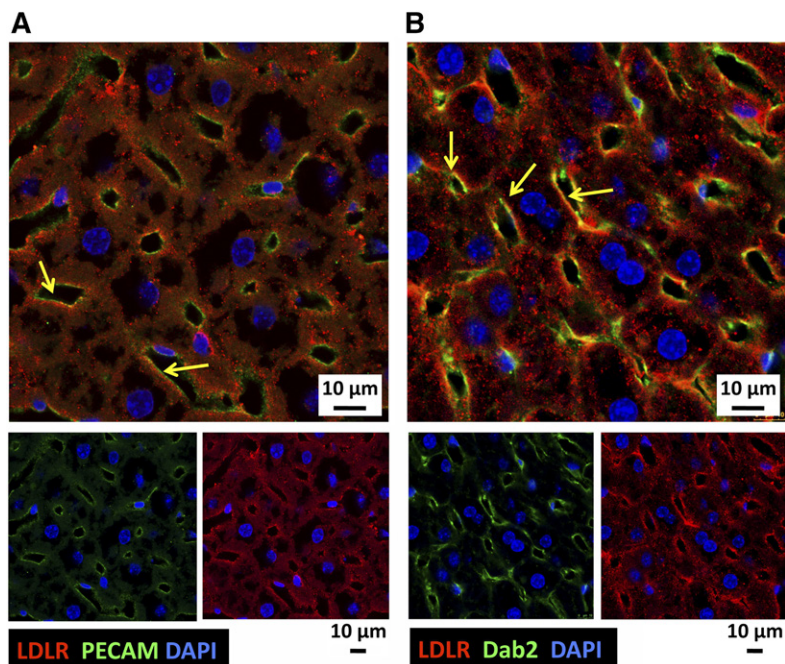


Fig. 7. Colocalization of Dab2 and LDLR in the sinusoidal endothelial cells of the liver. Cryosections of liver tissues from wild-type mice were analyzed by confocal immunofluorescence microscopy. A: Liver sections were stained for LDLR (red), PECAM (green), and DAPI (blue). B: Liver sections were stained for LDLR (red), Dab2 (green), and DAPI (blue). Enlarged images with overlaid signals are shown on top.

LDL uptake only through the sinusoid endothelial cells, and the derived cholesterol resides in a cellular pool that is able to regulate cholesterol synthesis in hepatocytes. We conclude that the concerted roles of Arh and Dab2 are responsible for the majority of adaptor function for LDLR endocytosis and LDLR-mediated cholesterol clearance from the circulation, as well as the regulation of cholesterol synthesis through controlling HMGCR expression.


One unexpected finding is that Dab2 is expressed only in sinusoid endothelial cells but not in hepatocytes or Kupffer cells. However, the majority of liver LDLR locates within the hepatocytes, and endothelial cells likely only contribute to a very minor level of receptor-mediated LDL uptake. In the absence of Arh, LDLR-mediated LDL uptake in liver presumably occurs only in the sinusoid endothelia supported by Dab2 but not in hepatocytes, and only at a very low level. Because Arh knockout mice have low hepatic HMGCR protein, cholesterol derived from Dab2- and LDLR-mediated uptake of LDL in the sinusoid endothelial cells must be able to suppress hepatic HMGCR. Despite an increased liver cholesterol level in either LDLR-null or Arh/Dab2 double-knockout mice, we observed that liver HMGCR expression was greatly induced, to a similar extent in both mutant mice. This is consistent with the finding that cellular cholesterol is compartmentalized, and only a certain pool of cholesterol is able to regulate HMGCR (32). Therefore, the endothelial cholesterol derived from LDL uptake likely is exchangeable with the hepatic pool of cholesterol that is capable in the feedback regulation of its *de novo* synthesis.

Dab2 gene ablation alone in mice has a relatively minor impact on serum cholesterol, and the results suggest that Arh is the main LDLR endocytic adaptor involved in the clearance of circulating LDL in both liver and extrahepatic tissues and in the regulation of HMGCR for cholesterol synthesis. Because Arh knockout greatly affects serum

cholesterol but not hepatic HMGCR, Arh-mediated, but not Dab2-mediated, LDLR endocytosis is the main activity in the removal of circulating cholesterol. Hepatic cholesterol synthesis is only activated either in the absence of LDLR or by deletion of both Arh and Dab2.

The results from the double-knockout mice suggest that Dab2 plays a partially redundant or supplementary role to Arh in mediating LDLR endocytosis and is likely more relevant in regulating hepatic cholesterol synthesis through its function in sinusoid endothelia. Nevertheless, we did observe a significant increase in liver cholesterol content in Dab2 knockout animals, suggesting that Dab2 does impact LDL uptake through the liver sinusoidal endothelial cells and cholesterol synthesis despite the presence of Arh. The absence of both Dab2 and Arh in liver leads to greatly increased liver cholesterol to the level comparable to those of LDLR knockout, likely as a result of unsuppressed synthesis. Thus, the combined roles of Arh and Dab2 account for the majority of the requirement for LDLR endocytosis and clearance of circulating LDL in intact animals. Although extensive studies on the roles of Dab2 and Arh in LDLR endocytosis have been performed using cultured cells, the current study determined their roles in intact animals, particularly their impact on circulating cholesterol. This initial study limited the investigation to animals placed on a high-sucrose diet in the absence of dietary cholesterol. The mechanism would be expected to be much more intricate due to additional factors when the mice are on a diet of high fat and exogenous cholesterol (19–21).

This study brought new information to light regarding the roles of LDLR cellular endocytic trafficking in a whole organism and advanced the understanding of this complex but important issue of cholesterol metabolism. Several key genes including ARH, PCSK9, and Dab2 affect serum cholesterol levels by modulating the endocytosis and cellular trafficking of LDLR. The increasing

understanding of genes and cellular mechanisms impacting circulating cholesterol likely will be helpful to meet the challenge of the development of new drugs, biology-based practice of medicine, and formulation of guidelines for management of dyslipidemias and strategies to reduce cardiovascular diseases (3, 17, 33). 

The authors acknowledge technical assistance from Ms. Toni Yeasky; valuable comments from our colleagues, including Drs. Pedro Salas, Carlos Moraes, and Zafar Nawaz, and Jeffery Tse, for reading, suggestions, and comments on the project and manuscript; valuable assistance from the core facilities (Animal, Imaging, and Histo-pathology) at the University of Miami; and excellent assistance with confocal microscopy from Gabriel Gaidosh at the University of Miami Bascom Palmer Eye Institute Imaging Core Facility.

REFERENCES

- Goldstein, J. L., and M. S. Brown. 2015. A century of cholesterol and coronaries: from plaques to genes to statins. *Cell*. **161**: 161–172.
- American Heart Association. 1999. 1999 Heart and Stroke Statistical Update. American Heart Association, Dallas, TX.
- Expert Panel on Detection, Evaluation, and Treatment of High Blood Cholesterol in Adults. 2001. Executive summary of the Third Report of the National Cholesterol Education Program (NCEP) Expert Panel on Detection, Evaluation, and Treatment of High Blood Cholesterol in Adults (Adult Treatment Panel III). *J. Am. Med. Assoc.* **285**: 2486–2497.
- Gould, A. L., G. M. Davies, E. Alemao, D. D. Yin, and J. R. Cook. 2007. Cholesterol reduction yields clinical benefits: meta-analysis including recent trials. *Clin. Ther.* **29**: 778–794.
- LaRosa, J. C. 1992. Cholesterol and cardiovascular disease: how strong is the evidence? *Clin. Cardiol.* **15** (Suppl. 3): 2–7.
- Brown, M. S., and J. L. Goldstein. 1984. How LDL receptors influence cholesterol and atherosclerosis. *Sci. Am.* **251**: 58–66.
- Brown, M. S., and J. L. Goldstein. 1986. A receptor-mediated pathway for cholesterol homeostasis. *Science*. **232**: 34–47.
- Osono, Y., L. A. Woollett, J. Herz, and J. M. Dietschy. 1995. Role of the low density lipoprotein receptor in the flux of cholesterol through the plasma and across the tissues of the mouse. *J. Clin. Invest.* **95**: 1124–1132.
- Schekman, R. 2013. Discovery of the cellular and molecular basis of cholesterol control. *Proc. Natl. Acad. Sci. USA*. **110**: 14833–14836.
- Davis, C. G., M. A. Lehrman, D. W. Russell, R. G. Anderson, M. S. Brown, and J. L. Goldstein. 1986. The J.D. mutation in familial hypercholesterolemia: amino acid substitution in cytoplasmic domain impedes internalization of LDL receptors. *Cell*. **45**: 15–24.
- Garcia, C. K., K. Wilund, M. Arca, G. Zuliani, R. Fellin, M. Maioli, S. Calandra, S. Bertolini, F. Cossu, N. Grishin, et al. 2001. Autosomal recessive hypercholesterolemia caused by mutations in a putative LDL receptor adaptor protein. *Science*. **292**: 1394–1398.
- Abifadel, M., M. Varret, J. P. Rabes, D. Allard, K. Ouguerram, M. Devillers, C. Cruaud, S. Benjannet, L. Wickham, D. Erlich, et al. 2003. Mutations in PCSK9 cause autosomal dominant hypercholesterolemia. *Nat. Genet.* **34**: 154–156.
- Cohen, J. C., and H. H. Hobbs. 2013. Genetics: Simple genetics for a complex disease. *Science*. **340**: 689–690.
- Leren, T. P. 2014. Sorting an LDL receptor with bound PCSK9 to intracellular degradation. *Atherosclerosis*. **237**: 76–81.
- Cohen, J., A. Pertsemlidis, I. K. Kotowski, R. Graham, C. K. Garcia, and H. H. Hobbs. 2005. Low LDL cholesterol in individuals of African descent resulting from frequent nonsense mutations in PCSK9. *Nat. Genet.* **37**: 161–165. [Erratum. 2005. *Nat. Genet.* **37**: 328.]
- Shapiro, M. D., S. Fazio, and H. Tavori. 2015. Targeting PCSK9 for therapeutic gains. *Curr. Atheroscler. Rep.* **17**: 19.
- Stone, N. J., and D. M. Lloyd-Jones. 2015. Lowering LDL cholesterol is good, but how and in whom? *N. Engl. J. Med.* **372**: 1564–1565.
- Mishra, S. K., S. C. Watkins, and L. M. Traub. 2002. The autosomal recessive hypercholesterolemia (ARH) protein interfaces directly with the clathrin-coat machinery. *Proc. Natl. Acad. Sci. USA*. **99**: 16099–16104.
- Jones, C., R. E. Hammer, W. P. Li, J. C. Cohen, H. H. Hobbs, and J. Herz. 2003. Normal sorting but defective endocytosis of the low density lipoprotein receptor in mice with autosomal recessive hypercholesterolemia. *J. Biol. Chem.* **278**: 29024–29030.
- Jones, C., R. Garuti, P. Michaely, W. P. Li, N. Maeda, J. C. Cohen, J. Herz, and H. H. Hobbs. 2007. Disruption of LDL but not VLDL clearance in autosomal recessive hypercholesterolemia. *J. Clin. Invest.* **117**: 165–174.
- Harada-Shiba, M., A. Takagi, K. Marutsuka, S. Moriguchi, H. Yagyu, S. Ishibashi, Y. Asada, and S. Yokoyama. 2004. Disruption of autosomal recessive hypercholesterolemia gene shows different phenotype in vitro and in vivo. *Circ. Res.* **95**: 945–952.
- Mishra, S. K., P. A. Keyel, M. J. Hawryluk, N. R. Agostinelli, S. C. Watkins, and L. M. Traub. 2002. Disabled-2 exhibits the properties of a cargo-selective endocytic clathrin adaptor. *EMBO J.* **21**: 4915–4926.
- Maurer, M. E., and J. A. Cooper. 2006. The adaptor protein Dab2 sorts LDL receptors into coated pits independently of AP-2 and ARH. *J. Cell Sci.* **119**: 4235–4246.
- Moore, R., K. Q. Cai, W. Tao, E. R. Smith, and X. X. Xu. 2013. Differential requirement for Dab2 in the development of embryonic and extra-embryonic tissues. *BMC Dev. Biol.* **13**: 39.
- Ishibashi, S., M. S. Brown, J. L. Goldstein, R. D. Gerard, R. E. Hammer, and J. Herz. 1993. Hypercholesterolemia in low density lipoprotein receptor knockout mice and its reversal by adenovirus-mediated gene delivery. *J. Clin. Invest.* **92**: 883–893.
- Yang, D. H., E. R. Smith, I. H. Roland, Z. Sheng, J. He, W. D. Martin, T. C. Hamilton, J. D. Lambeth, and X. X. Xu. 2002. Disabled-2 is essential for endodermal cell positioning and structure formation during mouse embryogenesis. *Dev. Biol.* **251**: 27–44.
- Morris, S. M., M. D. Tallquist, C. O. Rock, and J. A. Cooper. 2002. Dual roles for the Dab2 adaptor protein in embryonic development and kidney transport. *EMBO J.* **21**: 1555–1564.
- Yang, D. H., K. Q. Cai, I. H. Roland, E. R. Smith, and X. X. Xu. 2007. Disabled-2 is an epithelial surface positioning gene. *J. Biol. Chem.* **282**: 13114–13122.
- Folch, J., M. Lees, G. H. Sloane Stanley. 1957. A simple method for the isolation and purification of total lipides from animal tissues. *J. Biol. Chem.* **226**: 497–509.
- Tao, W., R. Moore, E. R. Smith, and X. X. Xu. 2014. Hormonal induction and roles of Disabled-2 in lactation and involution. *PLoS One*. **9**: e110737.
- Zhao, Z., S. Pompey, H. Dong, J. Weng, R. Garuti, and P. Michaely. 2013. S-nitrosylation of ARH is required for LDL uptake by the LDL receptor. *J. Lipid Res.* **54**: 1550–1559.
- Das, A., M. S. Brown, D. D. Anderson, J. L. Goldstein, and A. Radhakrishnan. 2014. Three pools of plasma membrane cholesterol and their relation to cholesterol homeostasis. *eLife*. **3**: e02882.
- Ridker, P. M. 2014. LDL cholesterol: controversies and future therapeutic directions. *Lancet*. **384**: 607–617.